

As explained in the text, peak temperature ( $T_{max}$ ) and pressure ( $P_{max}$ ) estimates were respectively obtained using the Raman spectroscopy of carbonaceous material method and by (1) measuring the maximum Si content of phengite, (2) calculating a P-T pseudosection using an average bulk rock composition representative of each zone of interest and (3) deriving  $P_{max}$  from the intersection of the Si content isopleth for phengite and  $T_{max}$  (see also Herviou et al., 2022).

### **PEAK TEMPERATURE ESTIMATION**

Raman spectra of carbonaceous material (RSCM), were obtained using a Renishaw inVia Spectrometer at ENS Paris. The excitation light was provided by a laser (Cobolt Fandango) at 514.5 nm and at a power of 50 mW, focused on the sample using a x100 objective (Leica). Ten to twenty-two spectra per sample were acquired in the 1000-2000  $\text{cm}^{-1}$  range; acquisition time was 3x10 seconds with 10% of the laser power following the spectral acquisition parameters of Beyssac et al. (2002). Peak position, baseline correction and band width were determined using Peakfit© software. Temperatures were determined using Lahfid et al. (2010) for the ~200 to 320°C temperature range and Beyssac et al. (2002) for the 330-640°C temperature range. Results are given in Table 2 of supplementary material 2.

### **PEAK PRESSURE ESTIMATION**

The Si content of phengite is known to be particularly dependent on pressure variations (Saliot and Velde, 1982) and can also vary depending on the rock composition. The rocks sampled in this study have been collected from areas only recording Alpine metamorphism (except for the Briançonnais sample from the RU transect). We therefore have attempted to track the most highly substituted phengite by identifying the earliest foliations and by analyzing the phengite by electron microprobe in these fabrics. Then, all the analyses have been carefully

examined in order to only keep those containing less than 15% of Xpyrophyllite, to avoid high Si values that are not recording the highest tschermak substitution. The maximum Si content ( $Si_{max}$ ) obtained is interpreted to represent a minimum peak pressure recorded during the metamorphic history of the rock, as some phengite could have been partly/totally re-crystallized during exhumation. Analyses of phengite chemical composition were performed at CAMPARIS (Sorbonne Université, Paris) using an electron microprobe (Cameca SX-100 and SX-Five). Point measurements were made using classical analytical conditions (15 kV acceleration voltage and 10 nA beam current allowing  $\sim 2 \mu m$  beam size in wave-length-dispersive spectroscopy mode) with diopside (Ca, Mg, Si),  $MnTiO_3$  (Mn, Ti), orthoclase (K, Al),  $Fe_2O_3$  (Fe), albite (Na) and  $Cr_2O_3$  (Cr) as standards to measure elements indicated in brackets. Representative electron microprobe compositions of phengite are presented in Table 3 of supplementary material 2.

In order to precisely constraint the peak pressure, we calculated P-T pseudosections using *Perple\_X* software (version 6.9.1; Connolly, 1990, 2005, 2009; Fig S1A, B and C). Pseudosection modelling have been made with one consistent thermodynamic dataset for the three zone, using an average bulk rock composition representative of each one. For our three representative metapelites the used thermodynamic database is Holland and Powell (1998) with its corresponding solution models (for chloritoid, garnet, carpholite, biotite, phengite) except for chlorite (Lanari et al., 2014). Calculations were performed in a  $Na_2O$ - $K_2O$ - $FeO$ - $MgO$ - $Al_2O_3$ - $SiO_2$ - $H_2O$  (NaKFMASH) chemical system.  $CaO$  is mostly restricted to carbonates and partially in lawsonite (only 1 sample of the Briançonnais in this study) and was therefore not considered in these calculations.  $MnO$ ,  $TiO_2$ ,  $Cr_2O_3$ ,  $P_2O_5$ ,  $SrO$  and  $BaO$  are minor and only present in accessory phases and they were therefore also neglected. Respectively, used bulk rocks composition (given in weight %) are 0.80  $Na_2O$ , 1.67  $K_2O$ , 4.48  $FeO$ , 3.91  $MgO$ , 8.33  $Al_2O_3$ , 69.46  $SiO_2$  and 15.00  $H_2O$  for the Briançonnais, 0.73  $Na_2O$ , 1.49  $K_2O$ , 3.19  $FeO$ , 2.64

MgO, 6.59 Al<sub>2</sub>O<sub>3</sub>, 74.05 SiO<sub>2</sub> and 10.83 H<sub>2</sub>O for the Piemont and 0.56 Na<sub>2</sub>O, 1.56 K<sub>2</sub>O, 6.67 FeO, 5.51 MgO, 8.91 Al<sub>2</sub>O<sub>3</sub>, 55.79 SiO<sub>2</sub> and 18.83 H<sub>2</sub>O for the Liguro-Piemont. Pseudosections were calculated in the P-T range of 1.0-2.5 GPa and 300-600°C to cover all potentially peak P-T conditions recorded by metamorphic rocks of the Western Alps.

Finally, the minimum peak pressure conditions of each sample were determined from the intersection of Si<sub>max</sub> values (along Si-in-phengite isopleths) and their respective T<sub>max</sub> estimates using RSCM, both plotted on the pseudosections (Fig S1).

## REFERENCES CITED

- Beyssac, O., Goffé, B., Chopin, C., and Rouzaud, J.N., 2002, Raman spectra of carbonaceous material in metasediments: a new geothermometer: *Journal of Metamorphic Geology*, v. 20, p. 859–871, doi:[10.1046/j.1525-1314.2002.00408.x](https://doi.org/10.1046/j.1525-1314.2002.00408.x).
- Connolly, J.A.D., 1990, Multivariable phase diagrams: an algorithm based on generalized thermodynamics: *American Journal of Science*, v. 290, p. 666-718, doi: [10.2475ajs.290.6.666](https://doi.org/10.2475ajs.290.6.666)
- Connolly, J.A.D., 2005, Computation of phase equilibria by linear programming: A tool for geodynamic modeling and its application to subduction zone decarbonation: *Earth and Planetary Science Letters*, v. 236, p. 524–541, doi:[10.1016/j.epsl.2005.04.033](https://doi.org/10.1016/j.epsl.2005.04.033).
- Connolly, J.A.D., 2009, The geodynamic equation of state: What and how: *Geochemistry, Geophysics, Geosystems*, v. 10, p. n/a-n/a, doi:[10.1029/2009GC002540](https://doi.org/10.1029/2009GC002540).
- Holland, T.J.B., and Powell, R., 2004, An internally consistent thermodynamic data set for phases of petrological interest: *Journal of Metamorphic Geology*, v. 16, p. 309–343, doi:[10.1111/j.1525-1314.1998.00140.x](https://doi.org/10.1111/j.1525-1314.1998.00140.x).

- Lahfid, A., Beyssac, O., Deville, E., Negro, F., Chopin, C., and Goffé, B., 2010, Evolution of the Raman spectrum of carbonaceous material in low-grade metasediments of the Glarus Alps (Switzerland): RSCM in low-grade metasediments: *Terra Nova*, v. 22, p. 354–360, doi:[10.1111/j.1365-3121.2010.00956.x](https://doi.org/10.1111/j.1365-3121.2010.00956.x).
- Lanari, P., Wagner, T., and Vidal, O., 2014, A thermodynamic model for dioctahedral chlorite from experimental and natural data in the system MgO–FeO–Al<sub>2</sub>O<sub>3</sub>–SiO<sub>2</sub>–H<sub>2</sub>O: applications to P–T sections and geothermometry: *Contributions to Mineralogy and Petrology*, v. 167, p. 968, doi:[10.1007/s00410-014-0968-8](https://doi.org/10.1007/s00410-014-0968-8).
- Saliot, P., and Velde, B., 1982, Phengite compositions and post-nappe high-pressure metamorphism in the pennine zone of the French Alps: *Earth and Planetary Science Letters*, v. 57, p. 133–138, doi:[10.1016/0012-821X\(82\)90179-0](https://doi.org/10.1016/0012-821X(82)90179-0).
- Whitney, D.L., and Evans, B.W., 2010, Abbreviations for names of rock-forming minerals: *American Mineralogist*, v. 95, p. 185–187, doi:[10.2138/am.2010.3371](https://doi.org/10.2138/am.2010.3371).

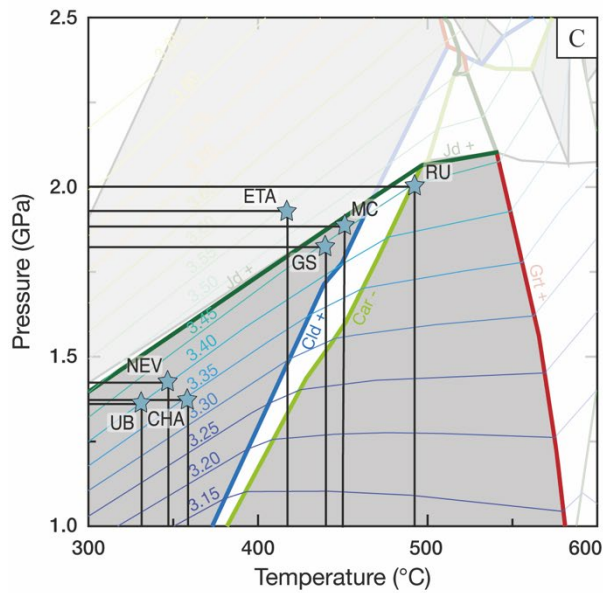
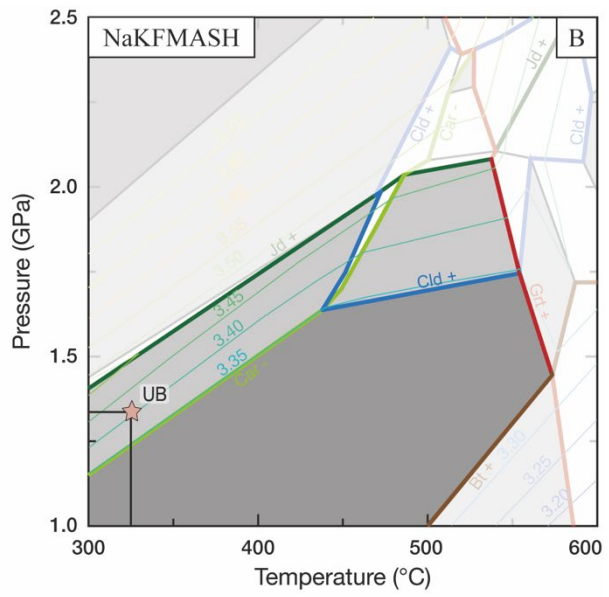
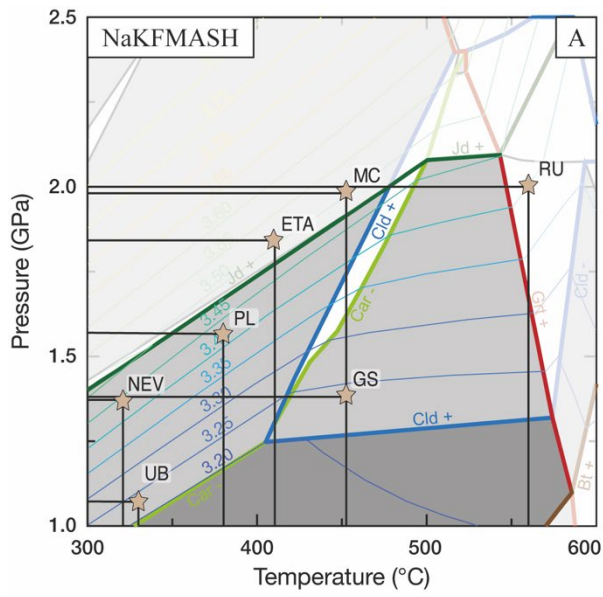


Figure S1: Pseudosection showing the intersection of the Si content isopleth for phengite and  $T_{max}$ . A: Briançonnais. B: Piemont. C: Liguoro-Piemont. See caption of figure 2 for abbreviation of samples and Whitney and Evans (2010) for minerals. Note that all field of interest contain phengite, chlorite, mica, quartz and  $H_2O \pm$  carpholite and chloritoid.

Samples data

Sample	Latitude	Longitude	Lithology	Mineralogy**	Temperature [°C]	Pressure [GPa]
Briançonnais						
RU	45,59724	7,03699	Quartzite	Qz-Ph-Chl-Grt	560	2.000
GS	45,48689	6,96117	Calcschist	Cb-Ph-Chl-Qz-Ep	459	1.380
GA	45,45606	7,04778	Marble	Cb-Qz	451	Ø
IS	45,43938	7,01126	Calcschist	Ph-Chl-Qz-Cb	419	Ø
PL	45,34097	6,87039	Calcschist	Ph-Chl-Qz-Cb	380	1.575
MC	45,22003	6,85358	Calc-schist	Ph-Chl-Qz-Cb	453	1.975
ETA	45,14893	6,80883	Calc-schist	Ph-Chl-Qz-Cb-Lws pseudo	412	1.800
NEV	45,04328	6,66367	Marble	Cb-Qz	318	1.375
CHA	44,95478	6,73642	Mica-schist	Ph-Qz-Chl-Grt	367	Ø
SV	44,68755	6,81023	Calc-schist	Ph-Chl-Qz-Cb-Lws pseudo	349	Ø
UB	44,60499	6,82539	Calc-schist	Cb-Ph-Chl-Qz	326	1.075
Piemont						
CHA	44,95617	6,73708	Marble	Cb-Qz	327	Ø
RB	44,81420	6,75754	Calc-schist	Ph-Chl-Cb-Qz	363	Ø
CQ	44,76394	6,79781	Calc-schist	Ph-Chl-Cb-Qz	358	Ø
SV	44,67625	6,85100	Calc-schist	Ph-Chl-Cb-Qz	309	Ø
UB	44,63957	6,86679	Calc-schist	Ph-Chl-Cb-Qz	338	1.340
Liguro-Piemont						
RU	45,62598	7,03224	Calc-schist	Ph-Chl-Cb-Qz	493	2.000
GS	45,49264	6,95544	Calc-schist	Ph-Chl-Cb-Qz-Ab	440	1.825
GA (GA2005 from Herviou et al., 2022)	45,45654	7,07285	Calc-schist	Ph-Chl-Qz-Ab-Cb-Lws pseudo	483	Ø
IS (49 from Gabalda et al., 2009)	45,41667	7,03333	Calc-schist	Ø	440	Ø
PL	45,32456	6,84919	Calc-schist	Cb-Ph-Chl-Qz	376	Ø
MC	45,20800	6,89917	Calc-schist	Ph-Chl-Cb-Qz	450	1.880
ETA	45,14940	6,80615	Calc-schist	Ph-Chl-Cb-Qz	417	1.875
NEV	45,07617	6,71278	Calc-schist	Cb-Qz-Ph-Chl	347	1.425
CHA	44,96303	6,77789	Calc-schist	Ph-Chl-Cb-Qz	358	1.375
RB	44,83358	6,80847	Calc-schist	Ph-Chl-Cb-Qz	370	Ø
CQ	44,75785	6,79218	Calc-schist	Cb-Ph-Chl-Qz	371	Ø
SV	44,68930	6,86560	Calc-schist	Ph-Chl-Cb-Qz	329	Ø
UB	44,61008	6,86842	Calc-schist	Ph-Chl-Cb-Qz	319	1.370

\*\* Abbreviation for minerals are from Whitney et Evans (2010).

## RSCM

Sample	Number of spectra	Température [°C]	Standard deviation T°	Standard error T°	R2	Standard deviation R2	Coefficient r <sup>2</sup>
Briançonnais							
RU	10	560	46	14	0,18	0,10	0,99
GS	20	459	13	3	0,41	0,03	0,99
GA	16	451	20	5	0,43	0,05	0,98
IS	16	419	7	2	0,50	0,02	1,00
PL	13	380	8	2	0,59	0,02	0,99
MC	21	453	16	4	0,42	0,04	0,99
ETA	16	412	6	1	0,51	0,01	0,98
NEV	20	318	10	2	0,63	0,01	0,99
CHA	15	367	14	4	0,62	0,03	0,99
SV	12	349	38	11	0,65	0,03	0,90
UB	15	326	18	5	0,64	0,01	0,99
Piemont							
CHA	14	327	20	5	0,71	0,05	0,90
RB	16	363	11	3	0,62	0,02	0,99
CQ	18	358	14	3	0,64	0,03	0,97
SV	16	309	34	9	0,62	0,03	0,99
UB	16	338	14	4	0,65	0,01	0,99
Liguro-Piemont							
RU	16	493	26	6	0,33	0,06	0,99
GS	14	440	21	6	0,45	0,05	0,99
GA (PL2001 from Herviou et al., 2022)	15	483	19	5	∅	∅	∅
IS (49 from Gabalda et al., 2009)	13	440	∅	4	0,45	0,03	∅
PL	16	376	7	2	0,59	0,02	1,00
MC	22	450	25	5	0,43	0,06	0,99
ETA	16	417	11	3	0,50	0,03	0,99
NEV	20	347	7	2	0,66	0,02	1,00
CHA	21	358	11	2	0,64	0,03	0,98
RB	20	370	6	1	0,61	0,01	0,99
CQ	16	371	16	4	0,61	0,04	0,98
SV	16	329	11	3	0,64	0,01	1,00
UB	13	319	11	3	0,63	0,01	0,99

## Microprobe analysis

Briançonnais								
Sample	RU	GS	PL	MC	ETA	NEV	/	UB
SiO2	50,76	47,64	51,31	53,07	53,31	52,78	/	48,16
TiO2	0,10	0,22	0,06	0,13	0,11	0,15	/	0,18
Al2O3	27,82	30,39	27,47	26,20	25,67	26,31	/	32,67
Cr2O3	0,04	0,01	0,03	0,03	0,02	0,03	/	0,00
FeOtot	3,11	2,82	3,30	4,20	2,74	0,56	/	1,31
MnO	0,04	0,03	0,00	0,02	0,07	0,00	/	0,01
MgO	2,52	2,71	2,85	1,94	3,89	6,21	/	1,88
CaO	0,03	0,00	0,03	0,06	0,03	0,04	/	0,08
Na2O	0,33	0,39	0,13	1,41	0,06	0,29	/	0,78
K2O	10,37	9,58	10,11	8,88	10,25	9,88	/	8,73
total	95,12	93,79	95,29	95,92	96,15	96,24	/	93,79
Si	3,40	3,23	3,42	3,51	3,51	3,44	/	3,22
Ti	0,01	0,01	0,00	0,01	0,01	0,01	/	0,01
Al	2,20	2,43	2,16	2,4	1,99	2,2	/	2,57
Cr	0,00	0,00	0,00	0,00	0,00	0,00	/	0,00
Fe	0,17	0,16	0,18	0,23	0,15	0,03	/	0,07
Mn	0,00	0,00	0,00	0,00	0,00	0,00	/	0,00
Mg	0,25	0,27	0,28	0,19	0,38	0,60	/	0,19
Ca	0,00	0,00	0,00	0,00	0,00	0,00	/	0,01
Na	0,04	0,05	0,02	0,18	0,01	0,04	/	0,10
K	0,89	0,83	0,86	0,75	0,86	0,82	/	0,74
XMg	0,59	0,63	0,61	0,45	0,72	0,95	/	0,72
Xprl	0,07	0,12	0,12	0,07	0,13	0,14	/	0,15
Xmu	0,52	0,61	0,50	0,31	0,43	0,41	/	0,61
Xcel	0,33	0,12	0,30	0,45	0,39	0,31	/	0,07
Xprg	0,04	0,05	0,02	0,18	0,01	0,04	/	0,10
Piemont								
Sample	/	/	/	/	/	/	/	UB
SiO2	/	/	/	/	/	/	/	50,27
TiO2	/	/	/	/	/	/	/	0,09
Al2O3	/	/	/	/	/	/	/	27,31
Cr2O3	/	/	/	/	/	/	/	0,01
FeOtot	/	/	/	/	/	/	/	2,46
MnO	/	/	/	/	/	/	/	0,04
MgO	/	/	/	/	/	/	/	2,96
CaO	/	/	/	/	/	/	/	0,01
Na2O	/	/	/	/	/	/	/	0,22
K2O	/	/	/	/	/	/	/	10,29
total	/	/	/	/	/	/	/	93,65
Si	/	/	/	/	/	/	/	3,41
Ti	/	/	/	/	/	/	/	0,00
Al	/	/	/	/	/	/	/	2,18
Cr	/	/	/	/	/	/	/	0,00
Fe	/	/	/	/	/	/	/	0,14
Mn	/	/	/	/	/	/	/	0,00
Mg	/	/	/	/	/	/	/	0,30
Ca	/	/	/	/	/	/	/	0,00
Na	/	/	/	/	/	/	/	0,03
K	/	/	/	/	/	/	/	0,89
XMg	/	/	/	/	/	/	/	0,68
Xprl	/	/	/	/	/	/	/	0,08
Xmu	/	/	/	/	/	/	/	0,52
Xcel	/	/	/	/	/	/	/	0,33
Xprg	/	/	/	/	/	/	/	0,03
Liguro-Piemont								
Sample	RU	GS	/	MC	ETA	NEV	CHA	UB
SiO2	51,65	52,73	/	52,30	53,47	50,40	49,53	52,11
TiO2	0,22	0,11	/	0,16	0,16	0,11	0,12	0,07
Al2O3	26,68	27,64	/	27,4	24,65	26,35	28,11	29,13
Cr2O3	0,01	0,06	/	0,04	0,03	0,04	0,03	0,03
FeOtot	4,13	2,5	/	2,94	3,83	5,54	3,35	2,25
MnO	0,00	0,00	/	0,00	-0,03	0,01	0,00	0,00
MgO	2,73	3,54	/	3,22	3,65	3,2	3,00	2,76
CaO	0,02	0,09	/	0,03	0,12	0,07	0,02	0,04
Na2O	0,18	0,25	/	0,21	0,03	0,17	0,15	0,24
K2O	10,6	10,45	/	9,83	10,8	9,46	10,67	10,21
total	95,66	96,91	/	95,78	96,00	95,17	94,98	96,86
Si	3,45	3,44	/	3,46	3,54	3,40	3,34	3,40
Ti	0,01	0,01	/	0,01	0,01	0,01	0,01	0,00
Al	2,10	2,13	/	2,11	1,93	2,10	2,23	2,24
Cr	0,00	0,00	/	0,00	0,00	0,00	0,00	0,00
Fe	0,23	0,11	/	0,16	0,21	0,31	0,19	0,12
Mn	0,00	0,00	/	0,00	-0,00	0,00	0,00	0,00
Mg	0,27	0,35	/	0,32	0,36	0,30	0,30	0,27
Ca	0,00	0,01	/	0,00	0,01	0,01	0,00	0,00
Na	0,02	0,03	/	0,03	0,00	0,02	0,02	0,03
K	0,86	0,87	/	0,83	0,85	0,82	0,92	0,85
XMg	0,54	0,76	/	0,66	0,63	0,49	0,61	0,69
Xprl	0,12	0,10	/	0,14	0,14	0,16	0,06	0,12
Xmu	0,47	0,48	/	0,46	0,39	0,45	0,57	0,53
Xcel	0,33	0,35	/	0,32	0,41	0,25	0,28	0,28
Xprg	0,02	0,03	/	0,03	0,00	0,02	0,02	0,03